International Journal of Mathematical, Engineering and Management Sciences
Vol. 2, No. 1, 37–52, 2017
https://dx.doi.org/10.33889/IJMEMS.2017.2.1-004

Design and Reinforcement of a B-Pillar for Occupants Safety in Conventional Vehicle Applications

Aniekan Essienubong Ikpe[1], Ejiroghene Kelly Orhorhoro[2,*], Abdulsamad Gobir[1]

[1]Department of Mechanical Engineering
Coventry University, Priory Street, CV15FB, West Midlands, UK
[2]Cemek Machinery Company
Technology Incubation Centre, Federal Ministry of Science & Technology
Benin City, Edo State, Nigeria
**Corresponding author*: kelecom@yahoo.com

(Received September 9, 2016; Accepted September 19, 2016)

Abstract
This paper is focused on B-pillar design and reinforcement with certain criteria that the final reinforcement design weight does not exceed 6Kg and the maximum displacement must be less than 40mm on the application of 140KN load. Surface welding method was applied on the first and second design while spot welding was used for the third design, whereas, seam welding was applied on the fourth design which happened to have the least maximum displacement, least maximum stress and weight compared to the other designs. The welding methods applied in each of the design gave different displacement values with the fourth design showing the least maximum displacement of 13.8mm and the third design showing highest maximum displacement of 31.9mm, while there was proximity in displacement values obtained for the first design (15.2mm) and second design (16.4mm). Hence, for the purpose of design against unforeseen damages during side collision, auto manufacturers may consider employing seam welding techniques when manufacturing a B-Pillar for occupant safety.

Keywords: B-Pillar, Reinforcement, Welding, Vehicle, Safety

Nomenclatures

A	Cross sectional area of the B-Pillar (m^2)
C	Cracked length (m)
C	Distance from the neutral axis to the top of the beam (m)
D	Actual maximum displacement (m)
E	Young's modulus (N/m^2)
F	Bending stress (N/m^2)
I	Moment of inertia of the beam cross section (kgm^2)
K	Coefficient of deflection
K_{IC}	Fracture toughness ($MPa.m^{1/2}$)
L	Length of B-Pillar due to applied load (m)
M	Resultant moment stresses (N/m^2)
M_s	Span moment of the B-Pillar (Nm)
N	Factor of safety
S	Section modulus (N/m^2)
U_c	B-Pillar centre deflection (m)
Wl	Total load on the B-Pillar (N)
y	Mid plane of the B-Pillar (m)
σ_{max}	Maximum allowable stress (N/m^2)
M_{max}	Maximum bending moment (Nm)

Abbreviations

AEMDB	Advanced Euro Mobile Deformable Barrier
CAE	Computer Aided Engineering
ENCAP	European New Car Assessment Programme
ESC	Electronic Stability Control
FOS	Factor of Safety

International Journal of Mathematical, Engineering and Management Sciences
Vol. 2, No. 1, 37–52, 2017
https://dx.doi.org/10.33889/IJMEMS.2017.2.1-004

1. Introduction

The significance of high strength and rigidity are fundamental prerequisite for any vehicle occupant's cell, this cannot be overemphasized due to the protection it provides against accident, particularly side impacts which greatly rely upon rigidity of what is referred to as safety cage (Arbelaez, 2005; Scharff et al., 1990). Road safety report describes an occupant cell as a '*survival box'* and suggests that the survival of occupants involved in the circumstance of an accident depend highly on the strength of the cell which is a fundamental prerequisite for vehicle safety design (Azadi et al., 2010). Other factors such as bad design, wrong communication, wrong decision, risk taken etc. can equally lead to road accident. According to Ivan et al. (2015) causalities, communication, socioeconomic, and sociocultural issues are important to understand nature of risks and to make correct decisions. From this point of view, it imperative that the frame and other supporting parts of a vehicle be properly designed to ensure safety and prevent loss of life in the event of accidents. As shown in Fig. 1, there are three main pillars supporting the frame work of a typical vehicle and these includes A-pillar, B-pillar and C-pillar, but some vehicles with very large compartment has additional pillar supporting structure at its rare side known as D pillar (Anderson, 2005). Moreover, each of the aforementioned pillars found in a car plays a vital role in the performance of a car but the B-pillar is one of the most important vehicles supporting structure due to a number of reasons that will be reviewed in this paper.

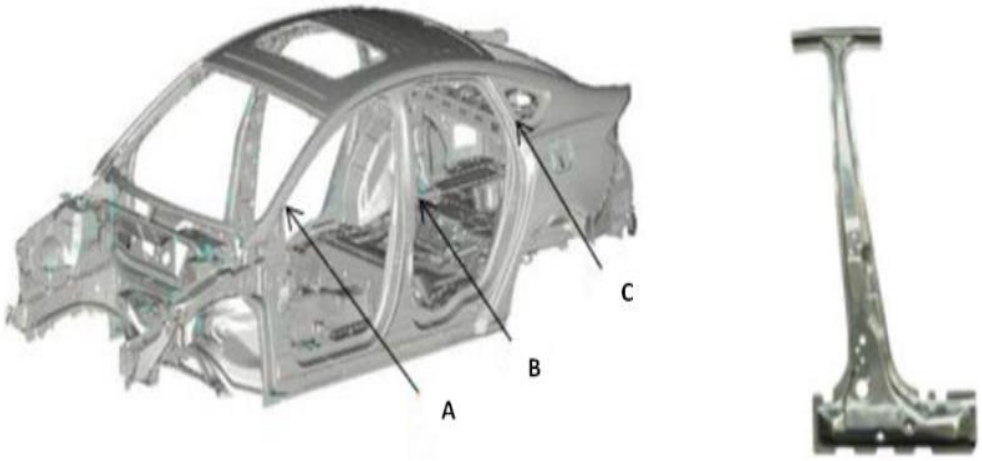

Fig. 1. A typical supporting pillars and their locations in a vehicle

The B-pillar also known as a "post" serves as a supporting member to a car's roof panel and it is also mounted sideward at the mid-section of a car for latching the front door and installation of the inches for the rare door (Ariffin et al., 2014). For installation purpose, B-pillar is a vertically closed steel structure welded to the vehicle's rocker panel and floor pan at the base and to the roof panel at the top. This paper focus mainly on the B-pillar and its relevance to a car when exposed to external force impacts caused by accidents or events that may affect the geometry of the car or occupants safety. As probably one of the most complex structural member that supports and maintains the geometry of a vehicle's roof, the B-pillar manufacturing may involve multi-layered assembly of various material strength and length (Tizzard, 1994). B-pillar is a very essential part of a car, and the stability of the occupant cell depends highly on the strength and rigidity of the pillar hence, necessitating proper design of the B-pillar for safety purpose against side collision or impact. However, some vehicles are manufactured without a B-pillar and these are known as

International Journal of Mathematical, Engineering and Management Sciences
Vol. 2, No. 1, 37–52, 2017
https://dx.doi.org/10.33889/IJMEMS.2017.2.1-004

hardtops, which can be found in two or four doors such as sedans, wagons and coupes (Thomas and Jund, 2013), but designs that does not incorporate a B-pillar for roof support at the mid side section between the front and rare door can greatly improve occupant visibility, but equally requires under-body strengthening to ensure structural rigidity. Moreover, some cars such as Limousines have more than two B-pillars which may be designated as B1, B2 etc. as a result of its lengthy physique. Accident investigation by Carney, (2012) revealed that 1 out of 5 accident results in side impact which accounts for 75% of vehicle occupant injury. Hence, for protection of passengers in accidental scenarios, the B-pillar design and manufacturing must be in line with existing standards and techniques to enhance resistance to impact which may depend on a number of factors including material and welding techniques. Therefore, in order to validate the efficiency of a B-pillar for proper design and reinforcement, it is necessary for the design to be analysed by Finite Element Analysis (FEA) using appropriate Computer Aided Engineering (CAE) software. FEA is a numerically analysis techniques for structural engineering designs. This involves design with the aid of complex software and FEA solvers, which can be used in analysing the effect impacts, vibration stress, heat transfer etc. It functions as a mechanisms of linked points referred to as nodes which combined arrangements make up an element often referred to as a mesh (Roymech, 2016). As shown in Fig. 2, FEA analysis are used for the development, improvement and analysis of structural components like the B-pillar with regards to the mesh size, design, material, displacement and stress analysis, location of welding areas. This paper also aims at analysing impact scenarios for a specific load case on the B-pillar without reinforcement and with reinforcement to determine the displacements, stresses and weight.

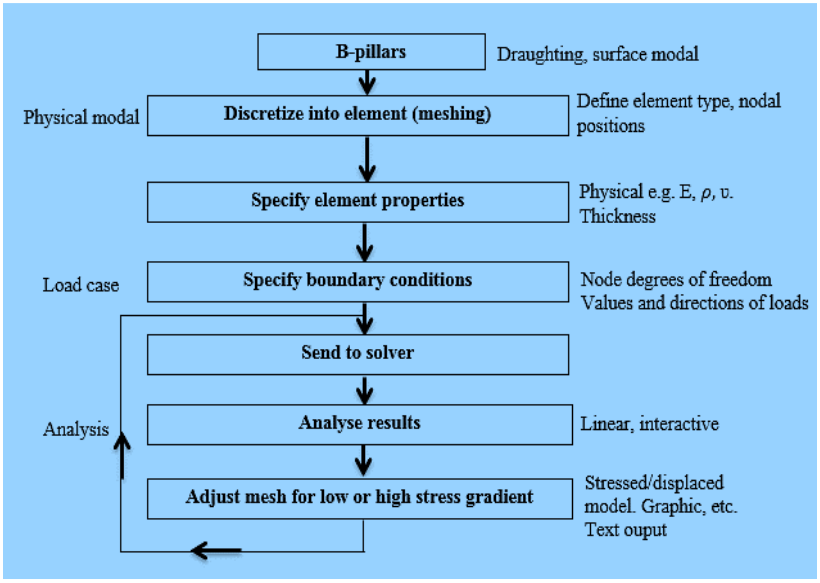

Fig. 2. Shows the representation of a typical flow procedure on FEA and modelling (Roymech, 2016)

Fig. 2 represents a typical procedure on FEA and modelling of the B-pillar. The first stage involves defining the geometry of the B-pillar for instance, followed by meshing process to determine appropriate mesh size, implementing the component properties, specification of boundary conditions, computing with FEA solver, result analysis, adjustment and readjustment of mesh sizes to achieve a good stress gradient for more accurate results. All these procedures will be employed in the analysis of the B-pillar in the reinforced and non-reinforcement state.

International Journal of Mathematical, Engineering and Management Sciences
Vol. 2, No. 1, 37–52, 2017
https://dx.doi.org/10.33889/IJMEMS.2017.2.1-004

2. Features of the B-Pillar

The B-pillar is made up of various symmetrical or structural components. Although the B-pillar design varies depending on the manufacturers, for interest of occupant protection in event of lateral impact or accident in the side direction, it is important to note that a vehicle structure still consist of other component which form part of the protection structure and these includes the C-pillar, A-pillar, rocker panel, floor pan, roof panel etc. as illustrated in Fig. 3. As mentioned earlier, one major advantage of the B-pillar is the provision of high level protection for passengers as well as the driver in cases involving intense side impact.

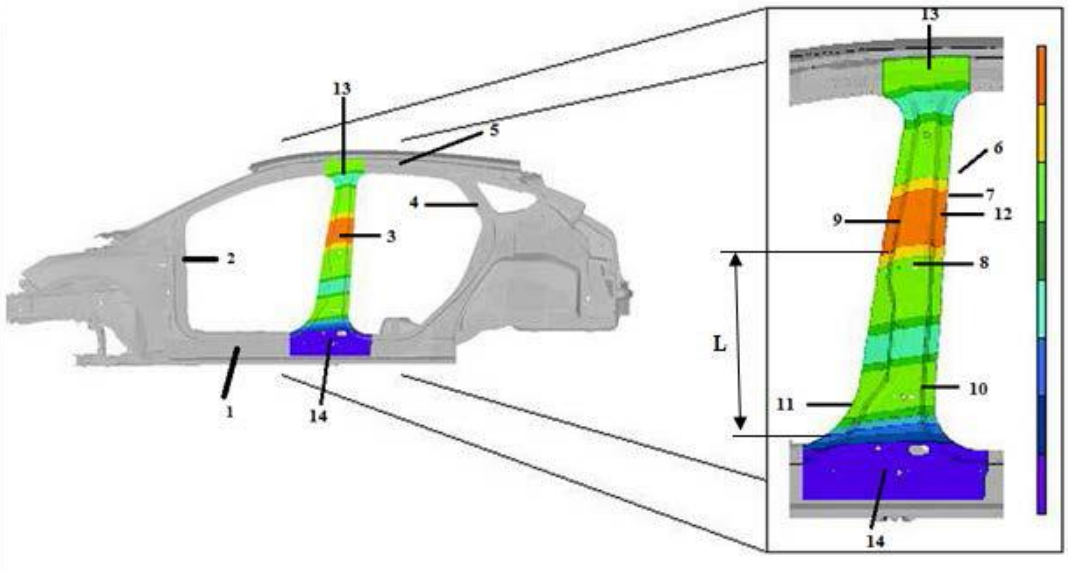

Fig. 3. The fundamental features of a B-pillar

Fig. 3 depicts the fundamental features of the B-pillar with regards to its position in the framework of direction of a vehicle structure, and side view. It also shows the connection or mating of the B-pillar with various other structural members to form a full lateral direction of an occupant cell. The A, B and C Pillars are designated (2), (3) and (4) and are attached together by the process of welding to the floor pan labelled as (1). Also, the roof rail or panel labelled (5) is welded to the uppermost end of the B-pillar. Furthermore, other parts of the B-pillar labelled 6, this consist of a curved-like member labelled (7), while the centre flange is labelled (8), the two web-like segments labelled (9) and 10 and both side flanges designated as (11) and (12). The lower and upper end section labelled (13) and (14) are the segments connecting the floor pan and the roof rail. Moreover, the length (L) signifies the softer area of lateral flanges 11 and 12 of the B-pillar. It is about 50% of the entire length of the flanges on the side (Hangs and Daniel, 2015). Moreover, Hangs and Daniel, (2015) indicated by shady part around the side flange which is the soft zone as well a variable depending on the requirement such as cover plate design and deformation properties. In crash cases involving side impact for example, the mid-section upper and base of the B-pillar are mostly affected, but good stiffness, fracture toughness and yield strength will minimize the chances of catastrophic failure under high loading impact. This is where the dissipation of impact energy is absorbed in form of plastic deformation which in turn improves the safety of the occupants of the vehicle (Hangs and Daniel, 2015). The aforementioned attributes describe the important functions and characteristics of a B-pillar. As

International Journal of Mathematical, Engineering and Management Sciences
Vol. 2, No. 1, 37–52, 2017
https://dx.doi.org/10.33889/IJMEMS.2017.2.1-004

mentioned earlier, the primary aim of a B-pillar is for occupant protection by minimising the accident effect or side impact damage, particularly when the direction of impact is sideward.

2.1 Standards for Side Impact of Vehicles

The analysis usually carried out for side impact on a vehicle before the parts are assembled is an example of a real life situation of accident scenario. This is carried out to determine the amount of force required to damage the B-pillar in such a manner that may severely affect the passenger sitting by the side. During the test procedures, if the B-pillar absorbs a certain amount of force without any serious damage to the car, such B-pillar can be considered suitable to protect passengers in incidents that involves serious side impact, but if the impact test proves otherwise, then more reinforcement has to be carried out before the vehicle parts are assembled. The impact test description is illustrated as shown in Fig. 4.

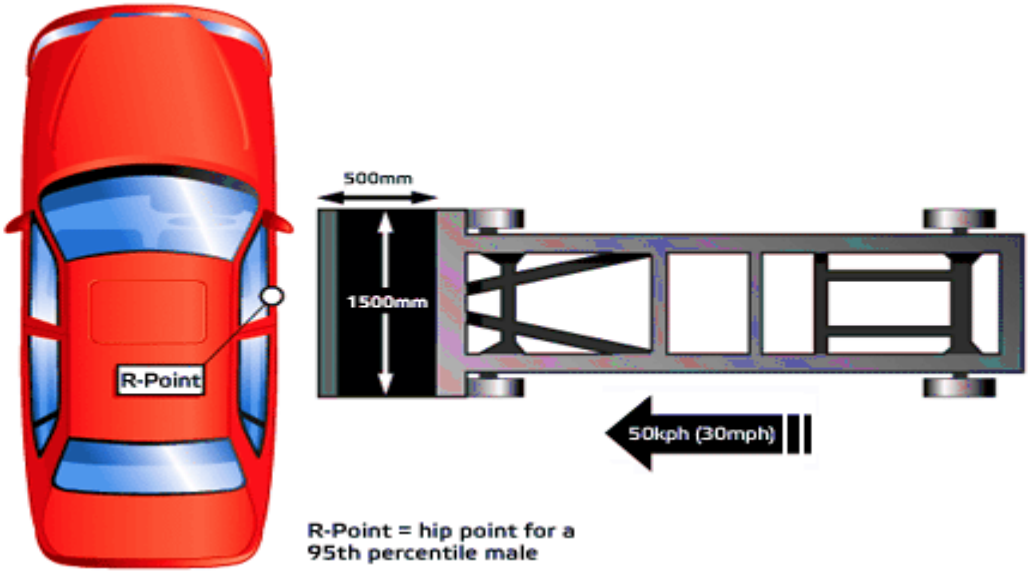

Fig. 4. Depicts procedure of car to car impact test (Hangs, and Daniel, 2015)

The impact test involves 500 X 1500mm impact requirements for the side collision on the driver of a fixed car at a speed of 50km/h as shown in Fig. 4, and this requirement in recent times has been improved of which now goes by the name Advanced Euro Mobile Deformable Barrier (AEMDB). The changes in dimension include 500± 2.5x1700±2.5mm in comparison to the other dimensions shown in Fig. 4 above (Euroncap, 2014). The Current Side impact test requirements for AE-MDB is listed as follows

(a) The static displacement of car must be 340± 20mm.
(b) The total speed of must be 50km/h.
(c) The dynamic peak displacement must be 346± 20mm
(d) The total weight must be 1300± 20kg.
(e) The movable barrier total energy absorption must be 61±5kJ.

Moreover, there are rules guiding the minimum standard requirement of new vehicles although to increase the safety standard of a vehicle or to ensure that the minimum requirement by law are

International Journal of Mathematical, Engineering and Management Sciences
Vol. 2, No. 1, 37–52, 2017
https://dx.doi.org/10.33889/IJMEMS.2017.2.1-004

met by vehicle manufacturing companies, numerous international organization responsible for monitoring and developing standard procedures for the impact test have evolved over the years to evaluate the safety of vehicles in the automotive industry. Some of this international organisation is European New Cars Assessment Programme (ENCAP). Over the years ENCAP has developed standards and procedures used in the evaluation and impact test analysis of conventional cars with the aim of improving vehicle behaviours against road accidents (Euroncap, 2014). ENCAP has developed numerous standards for testing and evaluating safety of vehicles before being sold out, some of which includes,

(a) Car to car side impact.
(b) Child protection.
(c) Frontal impact
(d) Seat belt reminder
(e) Pole side impact
(f) Autonomous emergency braking
(g) Pedestrian protection
(h) Speed assistance systems
(i) Whiplash
(j) Electronic stability Control (ESC)
(k) Meeting the Drivers

All the following represent the specific minimum requirements for assessing and testing the safety of a car during operation. It is imperative that side impact standards be considered as a guideline for FEA of a B-pillar, as this can provide details to the designer as to the amount of force that can affect the B-pillar performance, by so doing, the designer may consider reinforcing the B-pillar with suitable materials, and techniques. ENCAP standard evaluation of side impact suggests two methods namely; pole side impact and Car to Car side impact. The car to car side impact is illustrated in Fig. 4, where a simulation crash is carried out by a movable deformable barrier (Euroncap, 2014).

2.2 Initial Analysis of B-Pillar without Reinforcement

Table 1 shows the constraints in the geometries, load cases and material specification in the initial analysis of a B-pillar without reinforcement.

Total Height	Rake	Load Case
1000mm	120mm	140 KN Static Load

Table 1. Geometries and parameters of the B-pillar

Properties	Boundaries
Thickness	≤1.4mm
Density	7850kg/m^3
Yield strength	800MPa
Young's modulus	210GPa
Poisson's ratio	0.30
Tensile strength	1000MPa

Table 2. Specification of B-pillar material properties (CP Steel 800/1000)

International Journal of Mathematical, Engineering and Management Sciences
Vol. 2, No. 1, 37–52, 2017
https://dx.doi.org/10.33889/IJMEMS.2017.2.1-004

The maximum allowable thickness and young modulus is given as 1.4mm and 210Gpa, density of 7850kg/m³, poison ratio of 0.30 and tensile and yield strength as 1000 and 800MPa respectively.

2.3 Mesh Convergence Study

The given load case on the B-pillar for the initial analysis is depicted in Fig. 5. In the process of analysis the criteria were implemented on the B-pillar as required from the specifications shown in Table 2, the top end and base end were designed to dimensions of 160x40mm and 380x60mm respectively.

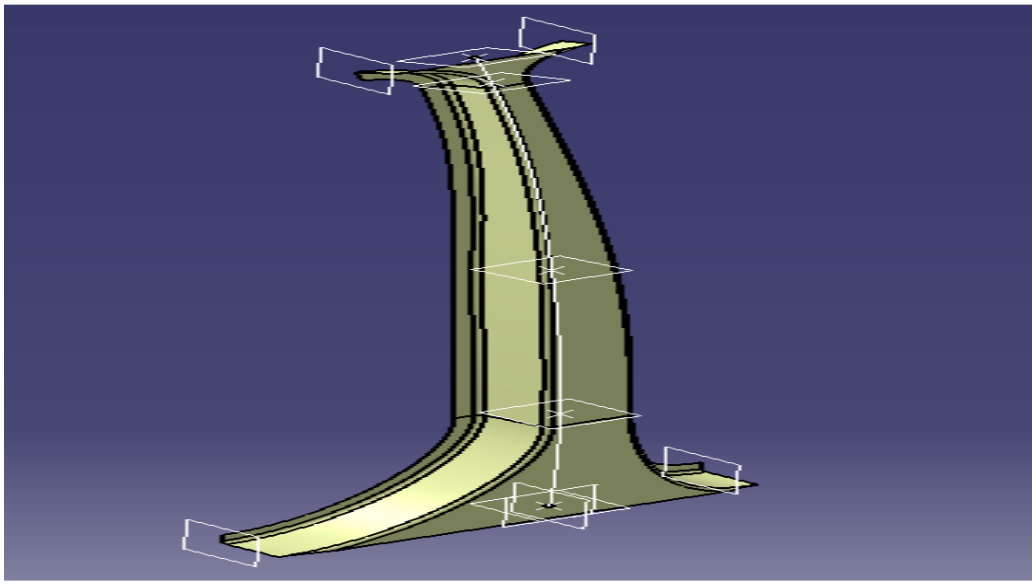

Fig. 5. Depicting the provided B-pillar for Analysis in the position load case

As discussed earlier, meshes are utilized in the process of FEA, where they are modelled to describe structural and material properties and their response under loading conditions. The major aim of carrying out modelling in FEA is to obtain accurate results for a certain load case, and for this to be achieved, it requires choosing a finer mesh size, although the computational time increases as the mesh size decreases. Therefore, to balance the computation time and accuracy of result, a mesh convergence study is required (Nafems, 2015). This process was carried out with a given load case (140KN) on the B-pillar, where it involved the use of varying mesh sizes starting from a higher mesh to lower mesh sizes which indicted a decrease in element distributions. In this case, a 2D triangular grids mesh was implemented. A convergence study of mesh sizes ranging from 10 to 2 mm was carried out. Result analysis and processing was done using Finite Element Analysis solver.

Mesh size	Von-Mises Stress (MPa)	Translational Vector Displacement (mm)
10	8.29×10^3	74.74
6	1.09×10^4	49.9
5	1.22×10^4	49.2
4	1.12×10^4	50.3
3	1.25×10^4	49.6
2	1.35×10^4	50.8

Table 3. Result of varying mesh sizes for 140KN load case

International Journal of Mathematical, Engineering and Management Sciences
Vol. 2, No. 1, 37–52, 2017
https://dx.doi.org/10.33889/IJMEMS.2017.2.1-004

It is important to note that the repetition of analysis is not solely for reliable and better mesh size, but to obtain accurate result of dense mesh size having considerably acceptable computing period. Apart from mesh size 10mm, subsequent meshes showed proximity for the von-mises stresses and displacements as shown in Table 3 and this signified that convergence has been reached and for this reason, there was no need for a convergence curve. Moreover, mesh size 3mm and 6mm showed very close proximity. Nevertheless, the solution is graphically presented in Fig. 6. This showed mesh convergence of varying mesh sizes specifically with respect to translational vector displacement.

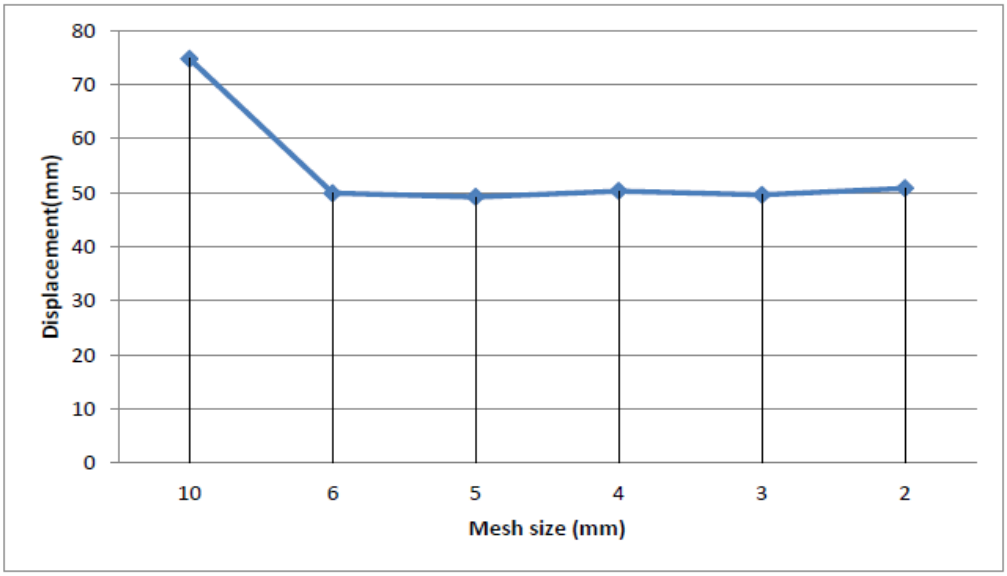

Fig. 6. Graph of displacement (mm) against mesh sizes (mm) for 140KN load case

From Fig. 6, convergence of magnitude of displacement can be noticed with increasing mesh size. 6mm mesh size displacement (maximum) of 49.9 and 3mm mesh size maximum displacement of 49.2 was recorded which signified that any of the two meshes can used to achieve similar solution for the model. Nafems, (2015) reported that the purpose of carrying out mesh convergence is to achieve smaller elements of the given model in such a way that the mesh size does not influence the solution of analysis. To ensure a more refined and accurate result for the given load case, a mesh size of 6mm was chosen for the final design of the FEA model. Mesh visualization is used for the given dimension of mesh as shown in Fig. 7.

International Journal of Mathematical, Engineering and Management Sciences
Vol. 2, No. 1, 37–52, 2017
https://dx.doi.org/10.33889/IJMEMS.2017.2.1-004

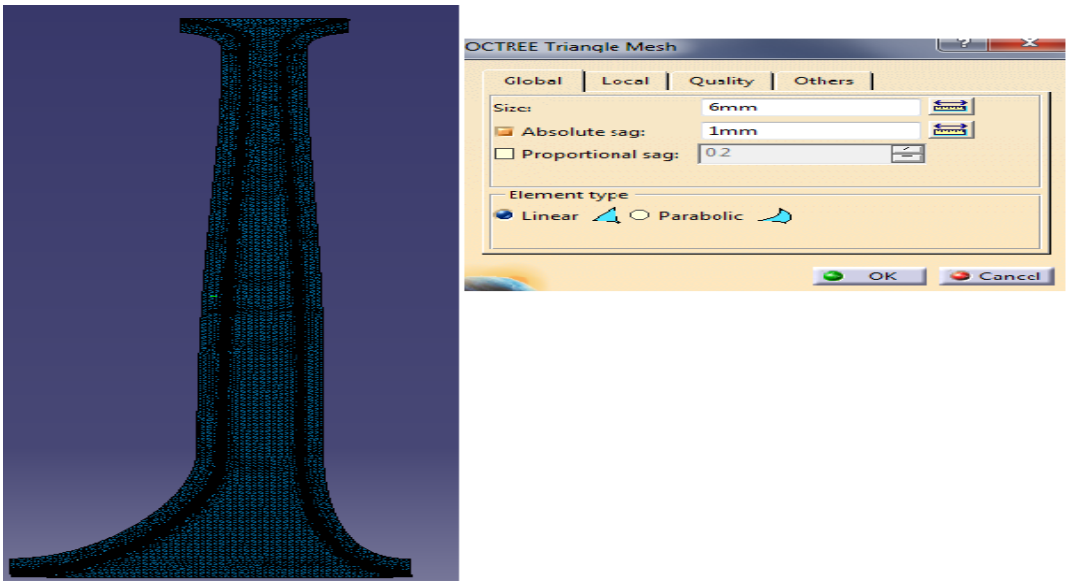

Fig. 7. Visualization of 6mm mesh selected

However, von-mises stress is another method of verifying or studying mesh convergence. Changes with steps in solution is presented in Fig. 8 for each element and a clear indication of the areas of higher stress gradient which B-pillars manufacturers must pay great attention to such areas, as they are prone to rapid deformation when exposed to side impact. Areas of high stresses and yield point can be identified in the B-pillar material by using different colours representing the von-mises stress values. For example, red colour represents the maximum stresses while blue colour signifies minimum stress as shown in Fig. 8. Furthermore, graphical contours can be used in the evaluation of the accuracy of mesh results, as it can indicate the areas that require localised mesh refining (Prosketch, 2014). Localised meshes are used where implemented mesh are not sufficient in certain areas of the model, this may be done to achieve a better solution at the end of the Finite Element Analysis. This can be adopted for 2-D and 3-D meshes.

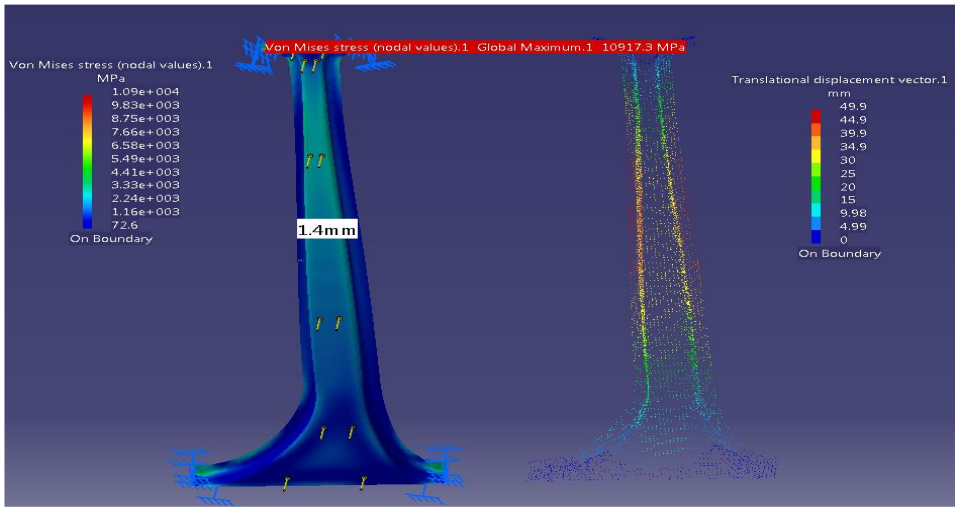

Fig. 8. Visualization of von mises stress and displacement on the B-pillar

International Journal of Mathematical, Engineering and Management Sciences
Vol. 2, No. 1, 37–52, 2017
https://dx.doi.org/10.33889/IJMEMS.2017.2.1-004

3. Design Considerations

Basic engineering design considerations were put in place to ensure that the B-pillar design meets the expected performance. The aforementioned design consideration is this discussed in details in this section.

3.1 Section Modulus

A beam under bending condition is exposed to high stresses at the axial fibres located far from the neutral axis. However, to prevent failure from taking place, large quantity of the beam material should be located in these areas where stresses are highly concentrated, while less material is required in the regions near the neutral. To design a symmetric I-beam to resist stresses resulting from the effect of bending, the first point of approach is usually the required section modulus. In cases where the maximum allowable stress σ_{max} and the maximum expected bending moment is M_{max}, the required section modulus (Gere and Timoshenko, 1997) can be expressed as;

$$S = \frac{M_{max}}{\sigma_{max}} = \frac{I}{c} \tag{1}$$

3.2 Bending Stress

The condition of the B-pillar is taken as a steal beam subjected to distributed load case for a static indeterminate beam and the B-pillar deflection under static load case is taken or referred to as B-pillar displacement. In addition, the steel beam theory of the mid span deflection for static indeterminate beams was used; this entails determining the second moment of area considering the b-pillar cross-sectional area of a particular surface where the load is exerted (Lie and Tingvall, 2012). The B-pillar bending stress for a given load case and displacement which is deflection, for instance deflection on the mid span was determined by;

$$\mathrm{U}_c = \frac{kM_s}{I} L^2 \tag{2}$$

$$\mathrm{f} = \frac{My}{I} \tag{3}$$

3.3 Fracture Toughness

Since flaws cannot be completely avoided during material selection, component design, processing, and fabrication, it is important to ensure that the manufactured component is stress free, as a little amount of stress induced in the component can propagate a pre-existing flaw, thereby, preventing the design from meeting its service life. However, the ability of a material to resist the presence of a flaw by the application of load that can result in brittle or ductile crack relates to material property known as fracture toughness which can be expressed as;

$$\mathrm{K}_{1\mathrm{c}} = \frac{wl}{A}(\pi c)^{0.5} \tag{4}$$

From equation 3, A is given as

$$A = \frac{wl}{\mathrm{K}_{1\mathrm{c}}} (\pi c)^{0.5} \tag{5}$$

International Journal of Mathematical, Engineering and Management Sciences
Vol. 2, No. 1, 37–52, 2017
https://dx.doi.org/10.33889/IJMEMS.2017.2.1-004

4. Final Design of B-Pillar with Reinforcement Plate

The material properties for both the B-pillar with reinforcement are shown in Table 4. This include restriction on geometric size and using a load case of 140N, combined mass of the reinforced B-pillar must be less than 6kg with maximum displacement below 40mm.

Additional Component	Reinforcement
Material	High strength alloy steel
Maximum Allowable thickness (mm)	2
Density (Kg/m^3)	7850
Young's Modulus (GPa)	210
Poison's ratio	0.3
Yield strength (MPa)	1500
Tensile Strength (MPa)	1700

Table 4. Material properties of the reinforced B-pillar

The key factor to be noted in a B-pillar reinforcement design is the stress and maximum displacement. Considering the given load case, weight is critical and must be considered as well as the factor of safety (FOS) which must be taken into account. In the B-pillar design, the factor of safety is taken as 2 which is based on the standard requirement for safety factors in existing practice and can be determined with the aid of yield strength (Roymech, 2016). A component is safe when the applied load does not surpass the inherent sustainable load. The factor of safety in this case can be expressed as

$$n = \frac{Maximum\ Load}{Actual\ Load} \tag{6}$$

The failure criteria is shows in Table 5.

Failure Criteria	Component Condition
$n = 1$	About to fail
$n < 1$	Fail
$n > 1$	Safe

Table 5. Indication of failure criteria (Roymech, 2016)

A factor of safety of 2 will be taken for the redesigned B-pillar the maximum displacement; Actual will be,

$$2 = \frac{40mm}{d}$$

Therefore, expected maximum displacement is d = 20mm

4.1 Design of the Main B-Pillar with Reinforcement

Many factors can influence the design model development of a B-pillar. Factors noted to influence the initial B-pillar design performance includes, second moment of area, factor of safety, dimension, position of constraints, assembly and manufacturability. Moreover, review was carried out on existing B-pillar designs from the different car models prior to developing and analyzing final model. The different B-pillar designs considered in this paper was based on

International Journal of Mathematical, Engineering and Management Sciences
Vol. 2, No. 1, 37–52, 2017
https://dx.doi.org/10.33889/IJMEMS.2017.2.1-004

displacement, weight, stress as shown in Fig. 9, 10, 11 and 12. Fig. 13 shows assembly of the final B-pillar reinforcement design while Table 6 shows the Results summary of all the Reinforcement Designs with Different Welding Methods.

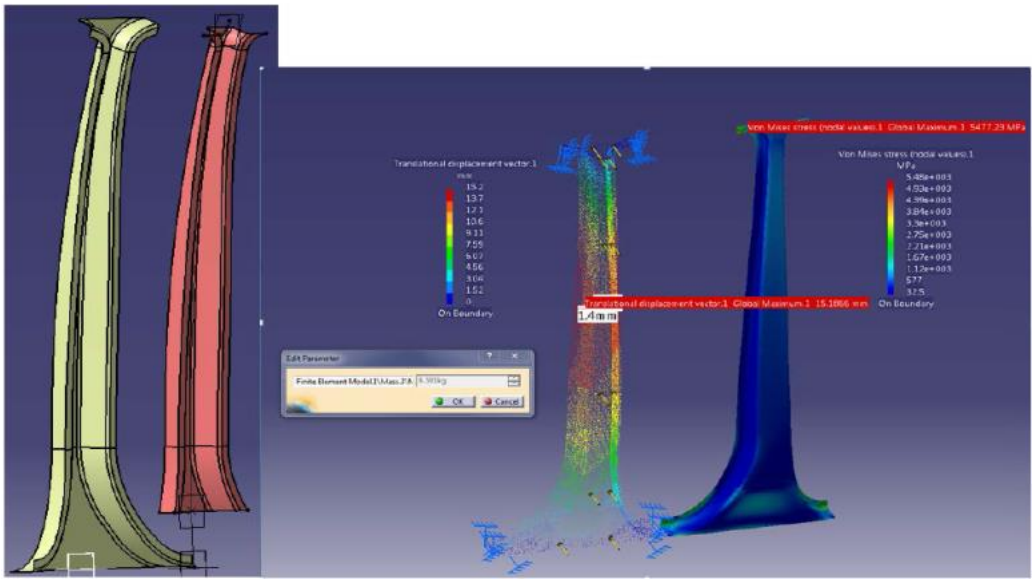

Fig. 9. Visualization of first design of B-pillar and results

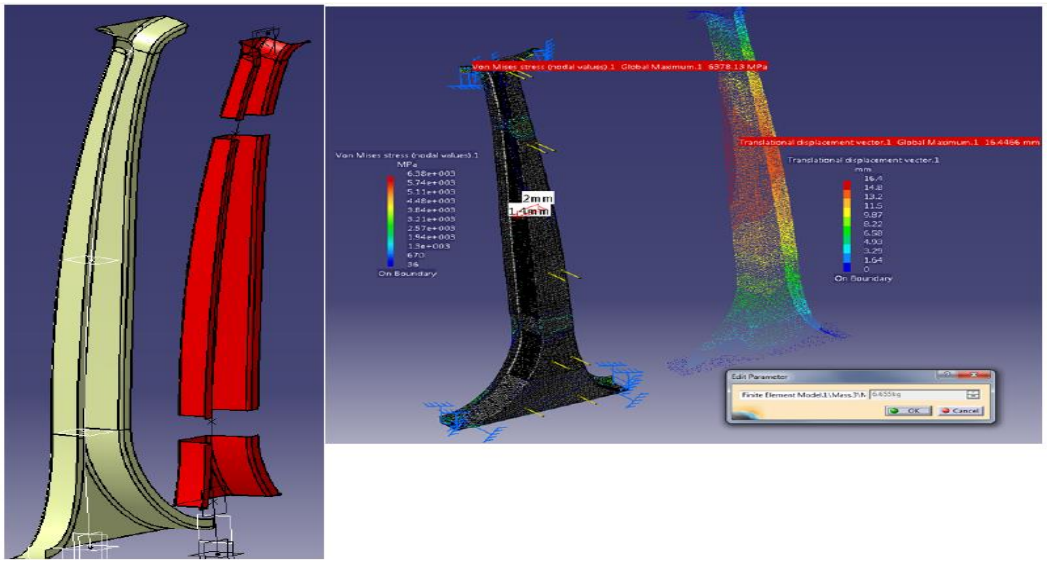

Fig. 10. Visualization of second design of B-pillar and results

International Journal of Mathematical, Engineering and Management Sciences
Vol. 2, No. 1, 37–52, 2017
https://dx.doi.org/10.33889/IJMEMS.2017.2.1-004

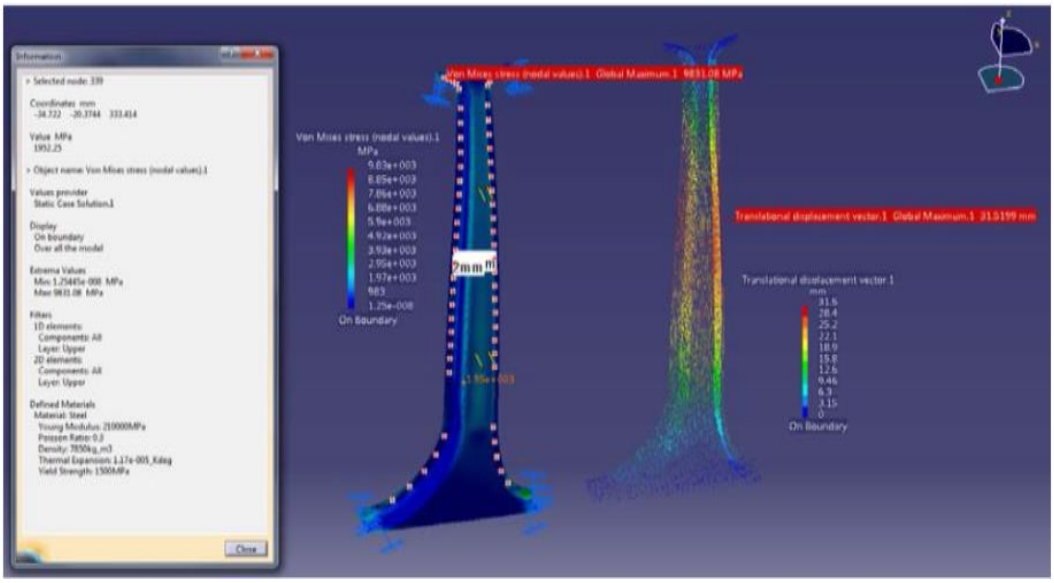

Fig. 11. Visualization of third design of B-pillar and results

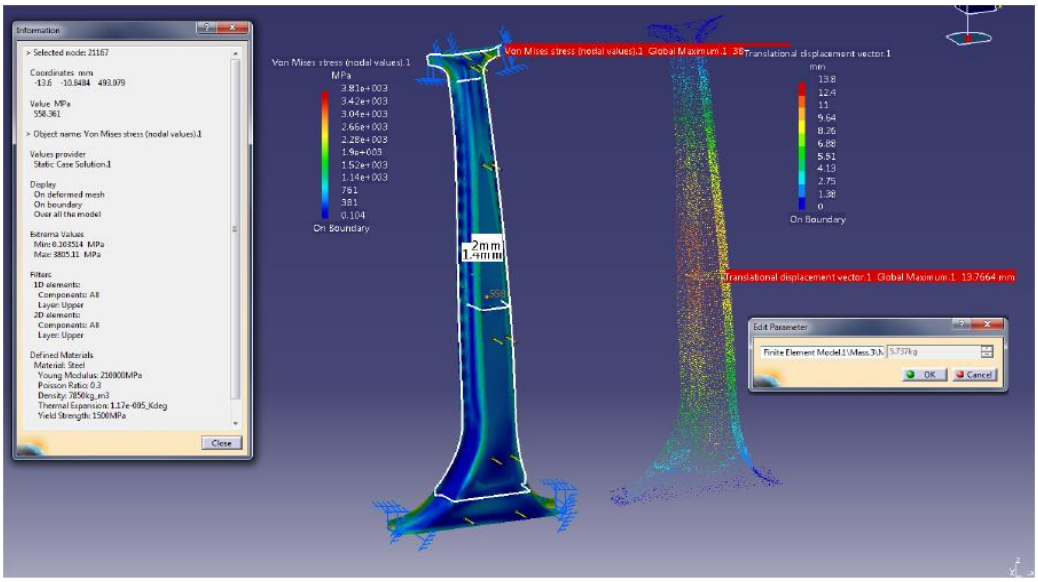

Fig. 12. Visualization of fourth design of B-pillar and results

International Journal of Mathematical, Engineering and Management Sciences
Vol. 2, No. 1, 37–52, 2017
https://dx.doi.org/10.33889/IJMEMS.2017.2.1-004

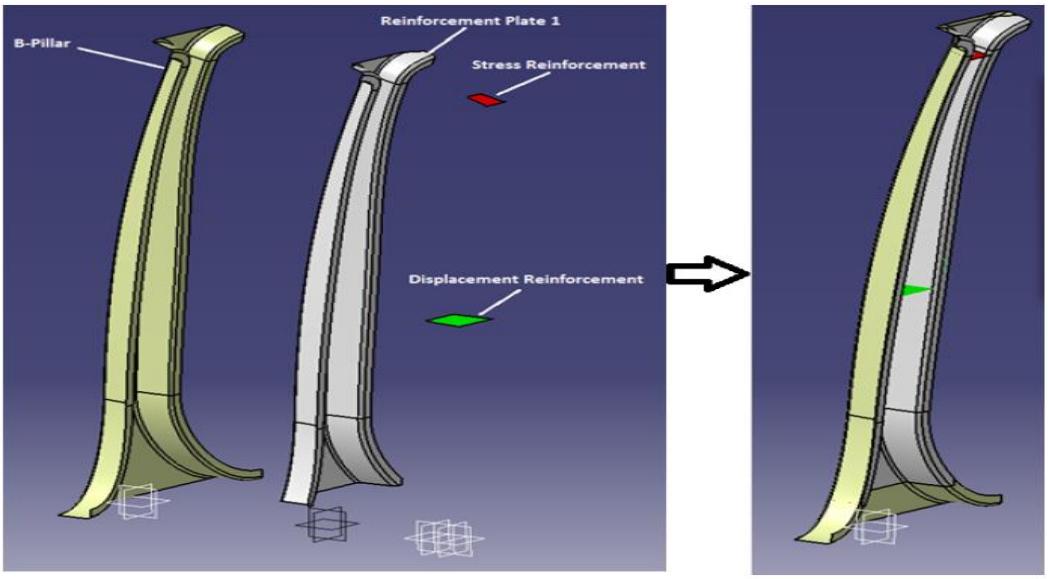

Fig. 13. Assembly of final reinforcement

Design	Maximum Displacement	Maximum Stress Value (Von-mises)	Weight (Kg)	Welding Method
1	15.2	5.48×10^3	6.591	Surface Welding
2	16.4	6.38×10^3	6.655	Surface Welding
3	31.9	9.73×10^3	5.921	Spot Welding
4	13.8	3.81×10^3	5.737	Seam Welding

Table 6. Results of reinforcement designs with different welding method

4.2 Discussion

Considering the various B-pillar reinforcement designs shown in Fig. 9, 10, 11 and 12, the forth design shown in Fig. 12 which was reinforced using seam welding techniques gave the least maximum displacement value, least maximum stress and the least density as shown in Table 6. Comparing the results obtained for each design as shown in Table 6, it was obvious that the fourth design met the specified requirements which will be further discussed in more details in this section. On the original B-pillar where convergence studies was carried out, 6mm mesh size was chosen for the reinforced design, due to a more accurate results and dense mesh size obtained by the 140KN load case. The final analysis of the FEA carried out with 6mm mesh size for 140KN load case was used in the B-pillar reinforcement designs shown in Fig. 9, 10, 11 and 12 respectively. As shown in Table 6, the maximum stress (for the fourth design which was chosen design) which is of great concern in this paper was noted as 3.18×10^3 MPa and the areas of high stresses was observed mostly on the edges of the lower and upper end of the pillar, where it was restrained with a clamp during the analysis as shown in Fig. 12. Apart from the areas of high stress concentrations, areas of very minimal stresses on the B-pillar is between 381 and 761MPa, which fell below the yield stress values and within the material elastic region. The colour illustration on the left hand side of Fig. 12 depicts the von-mises stress map of the result presented in Table 6, where red colours on the map represents the maximum stress level of

$3.81X10^3$ whereas, the blue colour represents the minimum stress level 381 and 761MPa respectively. Edges of the top hat section is consist of colours indicating stress values higher than 800MPa which is more than the yield point of the given material. Most of this stresses are concentrated at specific areas in the B-pillar and reinforcement which can be resolved by local meshing. The local meshing is generally used in solving stress concentrated related problems such as that of the B-pillar. Regarding the displacement obtained when a load of 140KN was applied on the B-pillar, a large region of the main body of the B-pillar recorded 11mm values while the mid-section of the B-pillar where the reinforcement plate extended across produced maximum displacement values of 13.8mm as shown in Fig. 12. The lower and upper ends of the B-pillar depicted no displacement at all. In conclusion on FEA carried out on the B-pillar reinforcement design, justification was drawn from the fact that displacement value less than 40mm and total weight less than 6Kg requirement for the chosen design was achieved. In the process of developing the reinforcement B-pillar design, a review was carried out on different shapes and design of the reinforcement plate. In addition, there was material restriction provided for the reinforcement as well as the moment of inertia, requires improvement as a result of observation. In initial B-pillar FEA result, for increased resistance against stress and displacement, a few sectional thin walled beam shapes were considered, specifically the I-beam. Various types of thin wall beam sections and their properties were considered in the B-pillar reinforcement plate. In the selection of sectional beam structure, the most important factor considered for reinforcement plate was simplicity. For structures like the B-pillar, simple design was considered for assembling, manufacturing and welding processes. Finally beam C-section structure was chosen with two additional stresses and displacement plate as a result of its simplicity, fitting into the geometry of the original b-pillar. Fig. 13 shows a complete assembly of the B-pillar reinforcement.

5. Conclusion

High strength to weight ratio plays a vital role in the design of automobile component, as automobile parts with this characteristic would not only improve vehicle performance but would as well reduce fuel consumption and CO_2 emission. The aim of the paper was to design and reinforce a B-pillar with certain criteria to withstand a load condition of 140KN, such that the weight does not exceed 6Kg, and the displacement must not be less than 40mm with the possible lowest stress on the application of 140Kg load. One out of four designs developed in this paper met the design requirements and can be adopted in design application of a B-pillar in real case scenario, provided the results obtained from the simulations are validated using other FEA solvers as well as hand calculations to fully ascertain the results before applying them on the real B-pillar design. Moreover, it was observed that stresses were found to be higher at the upper and lower end of the B-pillar which is the possible areas in the B-pillar that can deform most when exposed to severe side impact. For this reason, introduction of curves at sharp edges can minimise the stresses to some extent while extension of the reinforce material (plate) across the notches can as well minimise high stresses in such areas, thereby, optimising the B-pillar design for better performance.

References

Anderson, B. G. (2005). *Vehicle extrication: a practical guide*, PP. 141-143. PennWell Corporation, Oklahoma, USA.

Arbelaez, R. A. (2005). Side impact Challenges for steel Vehicle Structures. Insurance Institute for highway safety. Retrieved January 2, 2014, from

http://www.autosteel.org/~/media/Files/Autosteel/Great%20Designs%20in%20Steel/GDIS%202005/04%20-%20Side%20Impact%20Challenges%20for%20Steel%20Vehicle%20Structures.pdf.

Ariffin, A. H., Solah, M. S., Azhar, H., Isa, M., Hafzi, M., Rahman, M. K., & Anwar, K. (2014, September). Development of Mobile Deformable Barrier for Side Impact Crashworthiness Evaluation in ASEAN New Car Assessment Programme (ASEAN NCAP). In *Applied Mechanics and Materials* (Vol. 663, pp. 562-566). Trans Tech Publications.

Azadi, S., Vaziri, M., & Hoseini, M. (2010). Vehicle dynamic control of a passenger car applying flexible body model. *Vehicle System Dynamics*, *48*(5), 587-617.

Carney, D. (2012). The New Crash Test that will Change Your Next Car. Retrieved January 10, 2014, from http://www.popularmechanics.com/cars/a8070/the-new-crash-test-that-will-chang-your-next-car-11980742/.

Euroncap (2014). Car to Car Side Impact Euro NCAP - For safer cars crash test safety rating. Retrieved December 29, 2014 from <http://www.euroncap.com/Content-Web-Page/106f41f7-d486-46bf-bfbc-80fb4c79f679/car-to-car-side-impact.aspx.

Gere, J. M.; and Timoshenko, S. T. (1997). *Mechanics of materials. (4th ed.)*, ISBN: 9780534934293. PWS Publishing Company.

Hangs, B.; and Daniel, B. (2015). *B-pillar for a vehicle*. US 8292354 B2.

Ivan, K., Yuriy, V. K., and Otto, S. (2016). Land Use Drivers of Population Dynamics in Tasks of Security Management and Risk Assessment. *International Journal of Mathematical, Engineering and Management Sciences*, 1(1), 18–25, 2016.

Lie, A.; and Tingvall, C. (2012). How do Euro NCAP Results Correlate with Real-Life Injury Risk? A Paired Comparison Study of Car-to-Car Crashes. Retrieved January 2, 2015, from <http://www.euroncap.com/files/TIP_paper_2002---ea163391-0c67-4ad8-ae24-a176e39352f8.pdf> [2 January 2015].

Nafems (2015). NAFEMS The Importance of Mesh Convergence - Part 1 engineering analysis and simulation - FEA, Finite Element Analysis, CFD, Computational Fluid Dynamics. Retrieved January 2, 2015, from <http://nafems.org/join/resources/knowledgebase/001/.htm> [2 January 2015].

Prosketch (2014). Creating Octree 3D Mesh Parts. [online] Retrieved December 17th, 2014, from http://ps2.kev009.com/CATIAB18/cfyuganalysis_C2/cfyuganalysis3dmeshpart.htm.

Roymech (2016). Factors of Safety. [online] available from <http://roymech.co.uk/Useful_Tables/ARM/Safety_Factors.html> [2 January 2016].

Scharff, R., Mullen, K. and Corinchock J. A. (1990). *Complete automotive estimating*, pp. 172. Delmar Publishers, ISBN: 9780827335851.

Thomas, A., & Jund, M. (2013). *Collision repair and refinishing: a foundation course for technicians*. Delmar Cengage Learning.

Tizzard, A. (1994). *An introduction to computer-aided engineering*. McGraw-Hill.